Determination of the Structure of Polyelectrolyte Brushes

Y. Tran, P. Auroy,* and L-T. Lee†

Institut Curie, UMR 168, 11 rue Pierre et Marie Curie, 75231 Paris Cedex 05, France

Received March 24, 1999; Revised Manuscript Received August 31, 1999

ABSTRACT: We have prepared polyelectrolyte brushes on silicon blocks in two steps: first, we graft polystyrene (PS) chains terminated by a trichlorosilane group, and then, we convert the grafted PS to poly(styrenesulfonate, sodium salt) by using a soft sulfonation reaction. The grafted layers are fully characterized by ellipsometry and infrared spectroscopy. Using neutron reflectivity, we determine the interfacial density profile of the polyelectrolyte brushes so formed in aqueous solutions. In pure water, the chains are strongly stretched because of the electrostatic repulsion between charged monomers; the mean thickness of the brush is proportional to the chain length and does not depend on the grafting density. Upon addition of salt, two regimes are observed. As long as the salt concentration is less than the inner concentration of counterions in the brush ϕ_{ci}, the added electrolytes have no effect. On the other hand, if the salt concentration exceeds c_{ci}, the polyelectrolyte layer shrinks as the ionic strength increases but never collapses.

Introduction

Polyelectrolyte brushes are layers of charged polymer chains that are attached by one end on a flat surface (Figure 1). It has been thought that they could be used to protect surfaces against adsorption of various colloidal objects (such as proteins, polymers, and so on) to improve the stability of aqueous suspensions and so on. They could also be of some help to better understand the statistical physics of polyelectrolytes and the way some bacteria escape recognition by the immune system. The structure and properties of polyelectrolyte brushes have been the subject of extensive theoretical investigations during the past decade.[1−17] It has been shown that in a dense brush of (water-soluble) polyelectrolyte the chains are stretched due to the electrostatic repulsion between charged monomers. The brush thickness is determined by the balance between the chain elasticity and the osmotic pressure of the counterions. The effect of adding salt in solution has also been considered: polyelectrolyte brushes should be relatively insensitive to an increase in ionic strength, in contrast to most colloidal systems.

However, experimental studies of polyelectrolyte brushes are very scarce because of the extreme difficulty in preparing samples. Some authors have used diblock copolymers.[18−19] For instance, the adsorption of poly(*tert*-butylstyrene)−poly(styrenesulfonate sodium salt) (PtBS−NaPSS) block copolymers at a silica water interface has been investigated by Amiel et al.[18] The small hydrophobic PtBS block can be viewed as an anchor for the long hydrophilic NaPSS block, which is the charged, water-soluble chain. Among the results of this study, it has been shown that the adsorbed amount of the copolymer is significantly higher compared to that of the NaPSS homopolymer (of the same molecular weight) only when the concentration of salt added to the solution is high enough. Electrostatic interaction between monomers has to be screened sufficiently.[18] Free-standing black films obtained with this copolymer have also been studied.[20] By use of X-ray reflectivity,

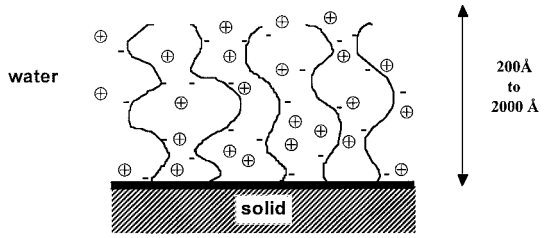

Figure 1. Schematic representation of the polyelectrolyte brush.

the film thickness (which is approximately twice the thickness of the polyelectrolyte brush) is measured as a function of the salt concentration. The results are in good agreement with theory. Chemically grafted polyelectrolytes have been synthesized and studied for the first time by Mir et al.[21] They used porous silica as substrate, on which they grafted polystyrene (PS) chains terminated by a reactive chlorosilane group. This neutral brush was then converted to a dense NaPSS brush by an in situ sulfonation reaction. The monomer density profile in aqueous solution was determined using small-angle neutron scattering. However, some limitations due to the synthesis (chain degrafting, insufficient analytical characterization) did not allow an exhaustive investigation: in particular, the influence of the molecular characteristics (chain molecular weight, grafting density and so on) was not systematically studied. The substrate (porous silica) was well adapted to neutron scattering but did not allow a precise control of the sample preparation.

Recently, the development of the "grafting from" techniques[22] has opened new possibilities for the preparation of polymer brushes. The synthesis of grafted polycation layers has been reported,[23] but a lot of work is still necessary to assess the meaning of these sophisticated methods.

In this study, we followed the same approach as did Mir et al.,[21] but we changed both the solid surface (which allowed us a much better control of the sample preparation) and the structural characterization technique. We chose silicon blocks as planar substrates to prepare NaPSS brushes. Using ellipsometry and infra-

† Laboratoire Léon Brillouin, CEN Saclay, 91191 Gif-Sur-Yvette Cedex, France.

10.1021/ma990443r CCC: $18.00
Published on Web 12/03/1999

red spectroscopy, we were able to control each stage of the brush preparation. The main characteristics of the samples were precisely measured: grafting density, sulfonation rate, and neutralization rate. Once the brushes were completely characterized, neutron reflectivity was used to determine the concentration profile of the brush in D_2O as a function of grafting density and chain length. The influence of the degree of sulfonation on the interfacial structure was also studied, even though this parameter could only be varied over a limited range because of the preparation method and the hydrophobic nature of polystyrene. The effect of ionic strength was also investigated by adding salt in solution.

In the next section, we will recall briefly the main theoretical investigations concerning polyelectrolyte brushes. In the Experimental Section, we will describe the synthesis and the characterization of samples. The neutron reflectivity method will also be explained. Then, the results obtained on polyelectrolyte brushes in pure water will be presented. From the density profile, the mean thickness is deduced and will be studied as a function of different parameters (sulfonation degree, grafting density, and chain length). The counterion distribution will also be determined. Finally, the influence of adding some salt into the bulk solution will be investigated.

Theory of Polyelectrolyte Brushes

Existing scaling theories give a large-scale description of polyelectrolyte brushes. In particular, the brush thickness is linked to the main molecular parameters (chain length, grafting density, and charge degree) and to the ionic strength by power laws.

The pioneering publication of Pincus[1] indicated different regimes corresponding to different counterion distributions. In this paper, the behavior of polyelectrolyte brushes in salt-free solutions is first considered. The brush thickness is determined from the balance between the osmotic pressure and the chain elasticity. In the *osmotic regime* that has been predicted for relatively dense and strongly charged brushes, the thickness is independent of the grafting density and satisfies the scaling law:

$$h \approx Na\alpha^{1/2} \tag{1}$$

where N is the polymerization index, a is the monomer size, and α is the fraction of charged monomers. In this regime, the mobile counterions are confined inside the brush, compensating the immobilized charge of the grafted chains. The latter are stretched because of the osmotic pressure due to the counterions. The *Pincus regime* corresponds to a sparse grafting of polyions and low degree of charge. In this situation, the counterion distribution extends into the bulk far beyond the brush because of the insufficient electrostatic attraction between the anchored polyions and the mobile counterions. The brush can be viewed as a simple charged surface and its thickness is now given by

$$h \approx 2\pi l_B \frac{a^2}{D^2}\alpha^2 N^3 \tag{2}$$

where l_B is the Bjerrum length ($l_B = 6$ Å in water) and D is the distance between two anchoring points ($\sigma = a^2/D^2$, the grafting density).

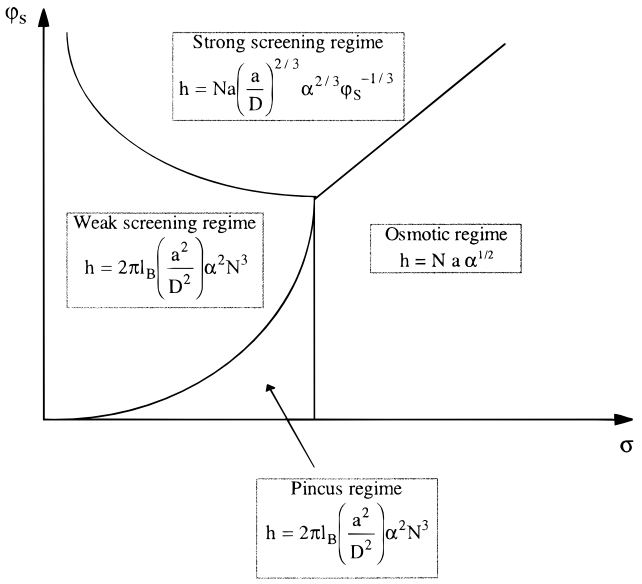

Figure 2. Diagram of states of a polyelectrolyte brush in the coordinates ionic strength vs grafting density. φ_S is the volume fraction of added salt, and σ is the grafting density.

The addition of salt to the bulk solution leads to the screening of the electrostatic interactions. In the "weak screening" limit, the added electrolytes disturb only the outer region of the brush whose thickness is the same as that in the Pincus regime. In the "strong screening" regime, Debye screening is expected to reduce the counterion osmotic pressure responsible for the chain stretching. The equilibrium condition gives

$$h \approx Na\left(\frac{a}{D}\right)^{2/3}\alpha^{2/3}\varphi_S^{-1/3} \tag{3}$$

where φ_S is the added salt volume fraction and a is supposed also to be the size of the counterion (and of any other electrolytes). Notice that the scaling law for polyelectrolyte brushes in the strong screening regime has the same form as the Alexander−De Gennes law for polymer brushes in good solvent.[24] A comparison with the osmotic regime shows that the brush shrinks when the salt concentration increases ($h \propto \varphi_S^{-1/3}$). However, even for high ionic strength, the chains remain as stretched as neutral chains in good solvent with an excluded volume parameter proportional to φ_S^{-1}: the brush is swollen by the excluded volume between counterions. The crossover between the osmotic regime and the strong screening regime occurs at $\varphi_S = \phi_{ci}$, where ϕ_{ci} is the inner concentration of counterions in the brush. For dense and strongly charged brushes, the osmotic regime is valid as long as φ_S is less than ϕ_{ci}. If the added salt concentration exceeds ϕ_{ci}, the added electrolyte screens the electrostatic interactions and induces a shrinkage of the layer. Wittmer and Joanny have recovered these scaling laws by considering a micellar solution of diblock copolymers adsorbed near a surface.[2] Their results are summarized by the diagram of states in the coordinates ionic strength versus grafting density shown in Figure 2.

Diagrams of states for the θ-solvent and the good solvent cases have also been presented.[4] The collapse of a planar polyelectrolyte brush caused by a decrease in solvent quality has been found to be a first-order conformational phase transition.[5−6] In addition, the influence of the substrate curvature has been consid-

ered: the conformation of polyelectrolytes grafted on spherical or cylindrical surfaces have been calculated.[7−8]

Self-consistent field (SCF) theories give access to the equilibrium structure of polyelectrolyte brush; in particular, they allow the determination of the monomer volume fraction profile. Misra et al.[10] have extended the SCF theory for neutral grafted chains[25] to charged brushes. Using the SCF approach and the local electroneutrality approximation, Zhulina et al.[11] have obtained analytical expressions for the density profile and the chain end distribution in the whole range of solvent quality and ionic strength. The local electroneutrality approximation assumes that the immobilized charges of the grafted chain backbones are locally compensated by mobile ions; it is hence applicable to relatively dense brushes. In salt-free solutions, the density profile (for a planar brush) has a Gaussian shape. In the strong screening regime, the profile shape tends to be parabolic at high ionic strength. Numerical results have been found to be in good agreement with these analytical predictions.[12] A similar approach has also been applied to the poor solvent case.[13] Recently, Borisov and Zhulina have developed the analytical SCF theory without any assumption about the distribution of mobile ions. Considering sparse brushes that are unable to retain their counterions, they found that a weakly charged brush has a stepwise density profile, in contrast to an "osmotic" brush (whose profile is Gaussian).[14−15] Finally, flow effects on polyelectrolyte brushes, in poor and good solvent, have also been examined.[16−17]

Experimental Section

In this paper, all of the interfaces are silicon-block−D_2O interfaces. The use of silicon blocks is a key point of this study: with these substrates, it is possible to analyze quantitatively the chemical modifications of the interface during the sample preparation by using a combination of two techniques (as described below): ellispometry and infrared spectroscopy in attenuated total reflection (IR-ATR). But these silicon blocks are also ideal substrates for neutron reflectivity, which is a powerful technique for determining the structure of a solid liquid interface.

Synthesis and Characterization of PSS^-Na^+ Brushes. Our strategy to synthesize a PSSNa brush on a silicon wafer is as follows: we use poly(styrene), terminated at one end by a reactive group that is able to form a covalent bond with the oxide surface of the silicon block; with this polymer, we build a dense brush of (neutral) polystyrene. This is followed by a soft sulfonation reaction performed directly on the brush to convert the neutral PS chains to polystyrenesulfonate.

Before use, the silicon block is cleaned for 20 min in a mixture of H_2SO_4/H_2O_2 (7:3) at 100 °C. This treatment eliminates all organic molecules present on the substrate surface and leaves the silicon block with a clean, hydrophilic oxide layer of about 20 Å thickness. The silicon block is rinsed with water in an ultrasonic bath and carefully dried under argon stream. Just prior to grafting, it is finally cleaned under UV ozone exposure (for 1 h).

The polystyrene is synthesized by anionic polymerization in benzene, by use of *sec*-butyllithium as initiator, and terminated by a trichlorosilane end-group.[26] The main characteristics of the PS used in this study are summarized in Table 1. For the grafting, the reactive PS is dissolved at 1% in carefully dried toluene; this solution is spread onto the silicon block, and the solvent is removed by either spin-coating or vacuum evaporation. The silicon block, covered by a thin layer of PS, is then immediately put in a vacuum oven, and the temperature is raised to 160 °C. Depending on the desired grafting density, the grafting reaction time is set between 5 and 24 h. Finally, the silicon block is thoroughly rinsed with toluene to eliminate all of the free chains that have not reacted.

Table 1. Main Characteristics of the Polystyrene Samples Used

H/D	M_W	polym. index, N	polydispersity
protonated	6550	63	1.16
protonated	12 550	121	1.08
protonated	32 250	310	1.04
protonated	114 020	1100	1.03
deuterated	4160	37	1.32

The thickness of the dry brush (which corresponds to the amount of PS per unit area) is measured by ellipsometry, from which the average distance D(Å) between anchoring points (or equivalently, the area per chain D^2, in square angstroms) is calculated. Therefore, with dry PS brushes, ellipsometry can be used to determine the number of $-CH_2-$ and aromatic $-CH-$ groups per unit area. This allows us to calibrate the IR-ATR technique: on the same samples, the IR absorbance at 2924 cm^{-1} (characteristic of $-CH_2-$) and the IR absorbance at 3026 cm^{-1} (specific of a monosubstitution of the phenyl ring) are measured, and thus, combining the two measurements, calibration curves of "absorbance versus number of groups per unit area" are obtained. It has to be noted that no orientation effect is detected on the IR spectra of the dry brushes, as it is commonly observed with short molecules,[27] because the order parameter in our grafted polymer samples is 2 orders of magnitude lower than that in self-assembled monolayers.

It was checked that the PS chains that are terminated by a trifunctional group $-SiCl_3$ do not form cross-linked aggregates during the grafting procedures we have used: the excess of free chains was analyzed by GPC after grafting, and the molecular weight distribution was found to be the same as that before. The dry PS brushes were also characterized by atomic force microscopy; they appeared as atomically smooth, homogeneous, and flat surfaces, with very rare holes. No clusters were detected. The holes however were useful: they allowed us to determine the thickness of the dry PS brush by AFM, and it turned out that this measurement was in complete agreement with the result obtained by ellipsometry.

The soft sulfonation reaction is adapted from Makowski et al.[28]: the sulfonation reagent, "acetyl sulfate", is prepared by slowly adding concentrated sulfuric acid to a solution of acetic anhydride (2.2 mol/L, 1.7 molar excess) in freshly distilled 1,2-dichloroethane, at 0 °C. The silicon block whose surface was grafted with PS is put in a specially designed reactor; the acetyl sulfate solution is introduced, the reactor is tightly closed, and the temperature is raised to 60 °C for 3−20 h. The poly(styrene sulfonic acid) so formed is neutralized rapidly by immersing the block in a 0.5 mol/L $NaHCO_3$ solution and rinsing it with pure water. A brush of poly(styrenesulfonate sodium salt) is thus obtained. The grafting density and the sulfonation degree of the polyelectrolyte brush are determined by comparing the IR spectra of the brush before and after sulfonation (see Figure 3). The adsorption band of the $-CH_2-$ group at 2924 cm^{-1} (or that of the aromatic $-CH-$ group at 3026 cm^{-1}) gives access to the rate of polymer degrafting (or, respectively, to the sulfonation rate). The neutralization rate is estimated using the signature of small counterions (tetramethylammonium or tetraethylammonium) other than sodium, which is not directly detectable in infrared spectroscopy. We take advantage of the sensitivity of the IR-ATR technique to the H/D substitution: we have synthesized deuterated PS chains (terminated by a trichlorosilane group), and we follow the same procedure as that explained above to obtain a deuterated polyelectrolyte brush. The last stage however is different: protonated tetraethylammonium (or tetramethylammonium) hydroxide is used as base (instead of sodium hydrogen carbonate). The neutralization rate corresponds to the ratio of the number of tetraethylammonium and the number of sulfonate groups per unit area, which are determined by the intensity of specific absorption bands (3010 cm^{-1} for the ethyl group and 2230 cm^{-1} for the aromatic $-CD-$ group). Comparison with bulk samples proves that the neutralization is complete in the polyelectrolyte brush.

Except for the study of the sulfonation degree influence on the brush structure, the reaction conditions have been opti-

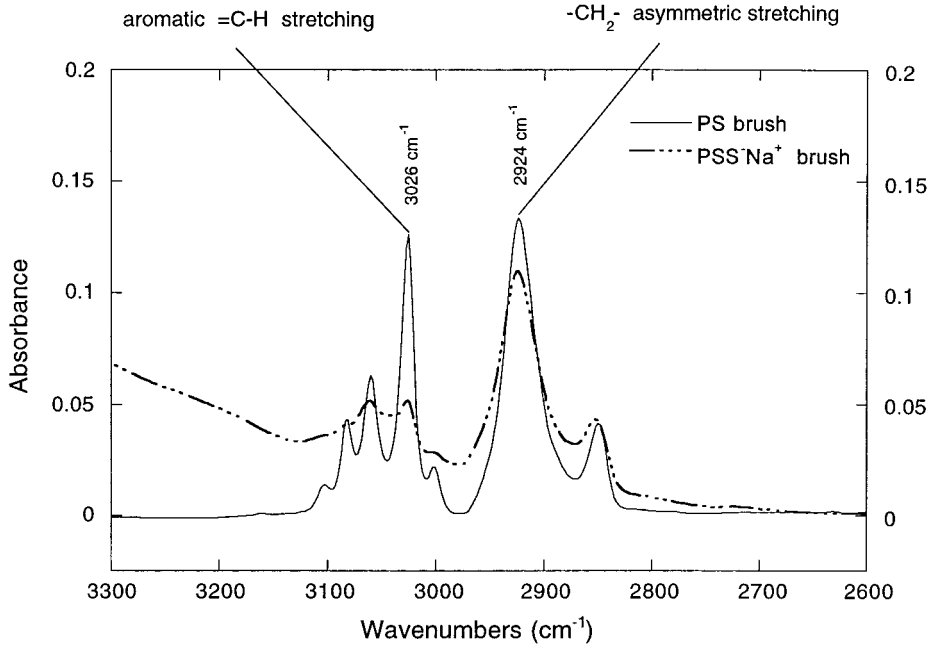

Figure 3. Comparison between the IR−ATR spectra of the same sample, before and after sulfonation. Solid line: PS brush (N = 310, D = 17.8 Å) before sulfonation. Dotted−dashed line: same brush converted to PSSNa after a 5 h sulfonation reaction. The absorption bands at 2924 and 3026 cm^{-1} are used to measure the polymer degrafting and the sulfonation rate.

Table 2. Brush Characteristics[a]

consolidation	polym. index, N	D before sulfon.[b]	sulfon. time[c]	D after sulfon.[b]	sulfon. rate, α
yes	1100	25.0	5	26.4	0.60 ± 0.08
no	310	17.8	5	22.0	0.62 ± 0.08
no	310	17.8	4	21.0	0.45 ± 0.10
no	310	17.8	3	20.0	0.35 ± 0.11
yes	310	17.8	5	21.2	0.60 ± 0.08
yes	310	21.2	5	23.0	0.60 ± 0.08
yes	310	25.6	5	27.0	0.60 ± 0.08
yes	310	27.5	5	29.0	0.60 ± 0.08
no	120	13.7	20	15.6	0.45 ± 0.10
no	63	12.4	20	13.0	0.45 ± 0.10

[a] For each chain length N, the experimental conditions have been optimized to have the maximum grafting density and the highest sulfonation rate. [b] In angstroms. [c] In hours.

mized in order to maximize the sulfonation rate and to minimize the degrafting of the polymer, which appears to be unavoidable. The reaction time that corresponds to the "optimal" sulfonation varies with the brush grafting density (cf. Table 2).

In addition, the homogeneity of the sulfonate group distribution along the backbone has been assessed by using a block copolymer. This question arises naturally because the sulfonation rate is not equal to 1. A diblock copolymer PS(D)−PS(H)$SiCl_3$ (number of deuterated (respectively, protonated) monomers N_D = 156 (respectively, N_H = 131); polydispersity index = 1.03) has been synthesized and grafted in the same way as that explained above to form a dense brush. After sulfonation, the sulfonation rate of each block (measured by IR-ATR) is found to be equal to that of the corresponding homopolymer. This indicates that the sulfonation is homogeneous along the backbone of the grafted PS chains.

Finally, we have observed that some PSSNa chains can be degrafted when the samples are immersed for a long time in water and especially when salt is added; in particular, brushes made with long chains (N = 1100) or of weak grafting density (D > 25 Å) appear to be fragile. The structure of these brushes cannot be determined by neutron reflectivity because the counting time is on the order of a few hours, which is too long to consider that the grafting density of these fragile samples remains constant. This difficulty has been solved by consolidating the grafted PS layer before sulfonation: the anchoring points are protected by tethering very short deuterated PS chains (N_D = 37). These oligomers are deuterated so that they can be distinguished from the protonated long chains in IR spectroscopy and neutron reflectivity. The amount of deuterated oligomers forming the protective carpet is measured by IR-ATR and ellipsometry; it decreases with the grafting density of the initial brush, from about 40 to 15 Å for the samples of this paper. This consolidating process appears to be very efficient: it reduces considerably the chain degrafting and allows us to prepare stable PSSNa brushes in a wide range of grafting density and chain length. More details about the synthesis and the characterization of PSSNa brushes will be given in a forthcoming publication. The main characteristics of the samples used in this paper are summarized in Table 2.

Neutron Reflectivity Experiments. Specular neutron reflectivity can be used to gain information about the structure of planar surfaces, both liquid and solid, at a mesoscopic length scale (from a few angstrom up to a few thousand angstroms). In particular, this method has been extensively used to characterize polymer interfaces.[29] Indeed, the specular reflectivity (which is the ratio of the reflected beam intensity and the incident beam intensity) is sensitive to the scattering length density profile (approximately, the equivalent of the refractive index for light reflectivity) in the direction normal to the interface Nb(z). In the kinematic approximation, the reflectivity $R(k)$ is linked to Nb(z) by

$$R(k) = R_F(k) \left| \int_0^\infty \frac{dNb}{dz} \exp(2ikz)\, dz \right|^2 \qquad (4)$$

k is the wave vector $4\pi \sin\theta/\lambda$, where λ is the neutron wavelength and θ is the angle of incidence. The Fresnel reflectivity $R_F(k)$ is the reflectivity of the bare surface. As $R_F(k)$ falls off sharply (it decreases asymptotically as k^{-4}), the R/R_F versus k representation will usually be preferred in order to emphasize the contribution of the scattering length density profile of the surface layer to the reflectivity signal. The power of the neutron reflectivity or scattering methods arises from the fact that the scattering length of hydrogen and deuterium is very different, whereas chemically, H and D can be considered as nearly equivalent. Therefore, selective deuteration can be used to highlight one particular component of the interface from others. To determine the polyelectrolyte brush profile in water, the polymer chains are protonated, whereas the solvent (D_2O) is deuterated. On the other hand, the

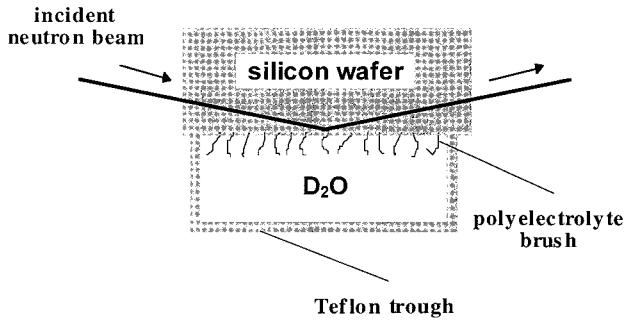

Figure 4. Schematic drawing of the neutron reflectivity experimental setup.

counterion distribution is investigated by contrast matching the grafted polymer backbone to the solvent: the counterions (tetraethylammonium) are protonated, whereas the poly(styrenesulfonate) is 96% deuterated, and the solvent is pure D_2O. Under this contrast matching condition, the neutrons are sensitive solely to the counterions.

The neutron reflectivity experiments were performed on the reflectometer DESIR at the Laboratoire Léon Brillouin, CE-Saclay (France). The sample holder keeps the silicon block (10 × 5 × 1 cm^3) tightly clamped against a Teflon trough filled with D_2O (or salted D_2O). The collimated incoming neutron beam traverses the silicon block (at a fixed angle), before reflecting at the silicon D_2O interface (Figure 4). Reflectivity was measured at a glancing angle of 1.2°, using neutrons of wavelength 3.5−22 Å. The reflectivity curves were normalized with respect to the plateau value corresponding to total reflection (observed for $k < k_c$, with k_c being the critical wave vector characteristic of the silicon D_2O interface). The experimental reflectivity curves were then analyzed as explained below.

The problem is to determine Nb(z) using eq 4. The method we have chosen[30] consists of approximating Nb(z) by a (fixed) number of layers of constant scattering length density, calculating the corresponding reflectivity curve and finding, by iterations, the parameters that best fit the experimental data. The adjustable parameters are the thickness h_i, the scattering length density Nb_i, and the roughness σ_i of the layer i. This roughness (of the error function type) allows one to connect two adjacent layers in a smooth way. Thus,

$$\mathrm{Nb}(z) = \sum_{n=0}^{N} \left(\frac{\mathrm{Nb}_i - \mathrm{Nb}_{i+1}}{2} \right) \left(1 - \mathrm{erf} \frac{(z - z_i)}{\sigma_i} \right)$$

with $h_i = z_i - z_{i+1}$. The first ($n = 0$) and last ($n = N$) layers are semi-infinite media. We have $Nb_{N+1} = 0$ and $Nb_0 = 2.0273 \times 10^{-6}$ $Å^{-2}$ (scattering length density of the silicon).

It appears that all our data can be fitted reasonably well using only four layers. No real improvement is obtained if this number of layers is increased up to 10, as shown by Figure 5. Although the fit seems to be better at large k (where the statistics is the worst), the density profile does not show any significant change. Among the four layers of the model, one describes the oxide layer, present at the surface of the silicon block. Its characteristics are determined before grafting and do not change for the rest of the experiment. Therefore, only three layers (nine parameters) are needed to describe the polymer interface.

The last operation of the method is to go from the scattering length density profile Nb(z) back to the density profile $\phi(z)$ of the protonated species. Usually, this is trivial. However, with our samples, we observed that a significant amount of H_2O introduces an additional difficulty. The presence of H_2O molecules has been detected by several methods. The PSSNa brushes, even "dry", exhibit an infrared absorption band characteristic of H bonds due to H_2O (between 3200 and 3600 cm^{-1}); cf. Figure 6. X-ray reflectivity experiments show that the electronic density is smaller than the density of pure PSSNa; it corresponds to the density of PSSNa with about 35%

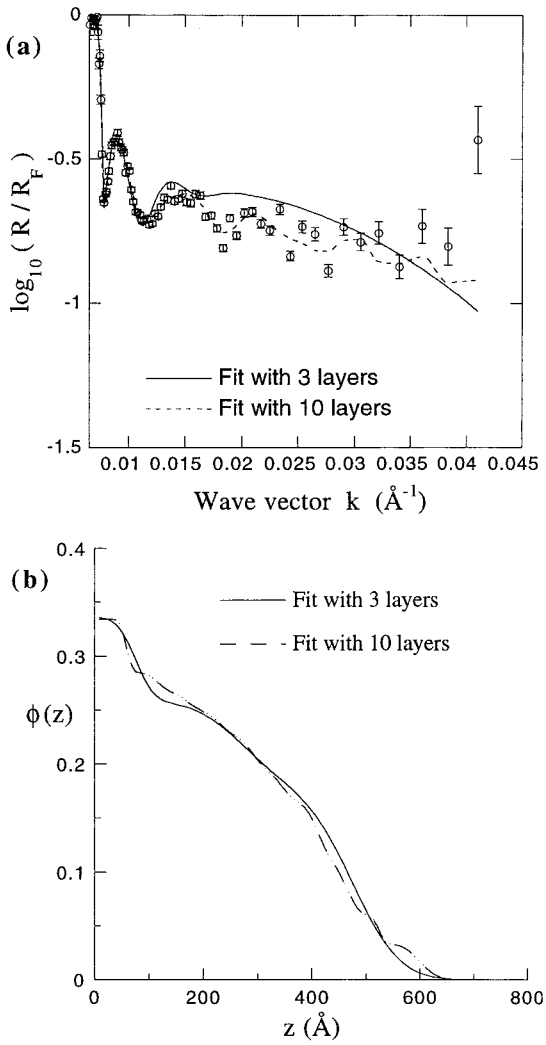

Figure 5. (a) Open circles: reflectivity data of a PSSNa brush ($N = 310$, $D = 22.0$ Å, $\alpha = 0.62 \pm 0.08$) in D_2O. The lines are the best fits corresponding to the reflectivity calculated with a model of 3 (solid line) or 10 layers (dashed line). (b) Similar monomer volume fraction profiles given by both fits.

H_2O. Finally, the neutron reflectivity curves of 96% deuterated brushes, which in principle are contrast matched with D_2O, are (slightly) different from the expected Fresnel reflectivity. If this difference is interpreted by the presence of H_2O within the polymer interface, we find again an amount of water on the order of 30%. This amount is, for all our samples, between 25% and 35%. These H_2O molecules cannot be removed even under high vacuum conditions nor can they be replaced by D_2O. They are introduced probably during the neutralization stage; they are strongly bound to the brush and presumably solvate the sulfonate groups.

If we assume that these H_2O molecules are distributed throughout the polymer interface in the same way as the sulfonate groups (or the counterions), then the unknown volume fraction of the protonated species can be obtained as

$$\phi(z) = \frac{\mathrm{Nb}_{D_2O} - \mathrm{Nb}(z)}{(\mathrm{Nb}_{D_2O} - \mathrm{Nb}_M) + w(\mathrm{Nb}_{D_2O} - \mathrm{Nb}_{H_2O})} \qquad (5)$$

w is the amount of H_2O and is precisely determined by comparing $\gamma = \int_0^\infty \phi(z)\, dz$ with the layer thickness measured by ellipsometry (which is the total amount of matter in the interface per unit area). (The z axis is oriented from the silicon block toward D_2O. The origin $z = 0$ for $\phi(z)$ is taken at the silicon oxide D_2O interface.)

A typical example of a reflectivity curve and the corresponding volume fraction that best fits the data, determined accord-

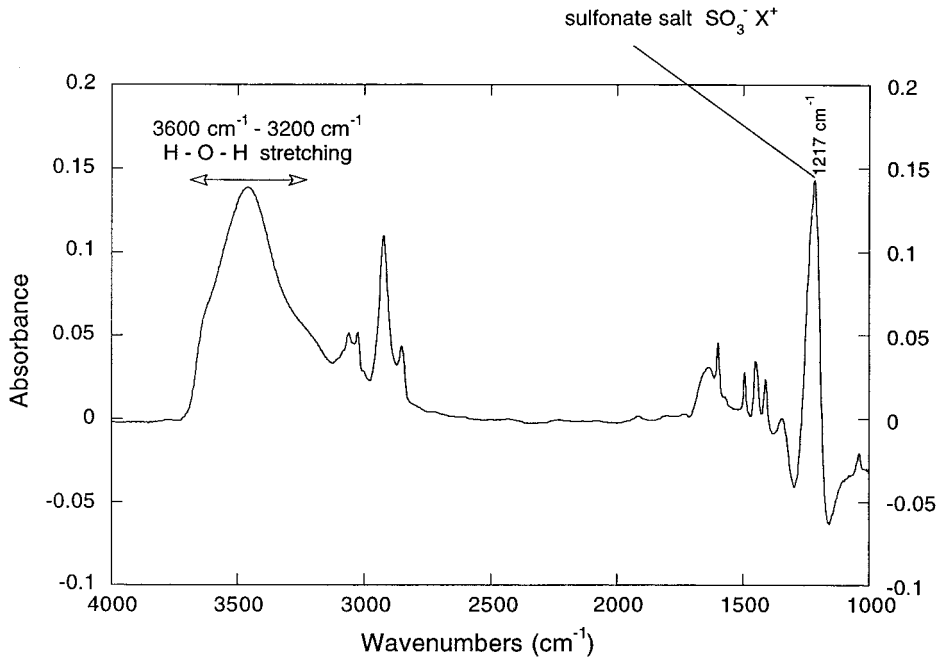

Figure 6. Typical infrared spectrum of a PSSNa brush. A broad absorption band characteristic of H bonds due to H_2O (3200−3600 cm^{-1}) can be observed.

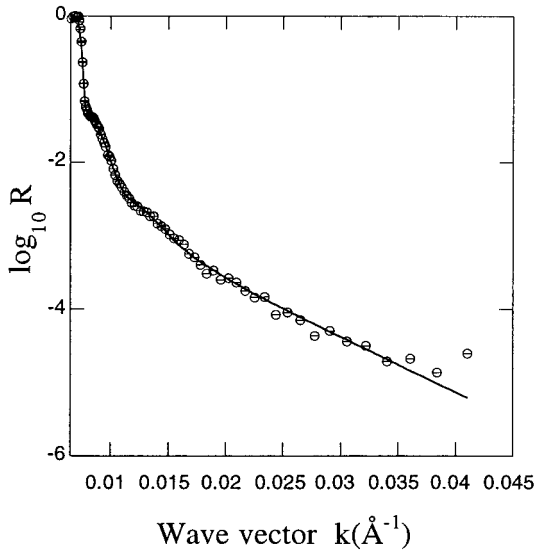

Figure 7. Same data as in Figure 5 but in the representation log R vs k. The solid line corresponds also to the best fit obtained with the three-layer model.

ing to the above-described procedure, was given in Figure 5 (solid line). In Figure 7, the same data are reported but in the representation log R versus k.

$\gamma = \int_0^\infty \phi(z)\, dz$ is an important physical parameter, because it does not depend on the shape of the density profile. Therefore, for a given sample, it should not vary from one experiment to another. For instance, if the ionic strength is changed, γ must remain the same even if the density profile shape completely changes. γ should also be the same when it is measured by different techniques. This parameter is thus a good tool to assess the meaning of the density profile $\phi(z)$ determined by neutron reflectivity.

To determine quantitatively the influence of the chain length, the grafting density, and so on and to compare the experimental results with theoretical predictions, it is useful to define the mean thickness of the brush h (Å) as $h = 2\int z\phi(z)\, dz / \int \phi(z)\, dz$. The maximum thickness h_{max} (Å), which corresponds to the z value where $\phi(z) < 0.01$, can also be used for the same purpose. Both are complementary ways to evaluate the chain extension.

Results

Influence of the Sulfonation Rate. Before studying the variation of the polyelectrolyte brush profile with grafting density and chain length, it was necessary to determine the influence of the sulfonation rate because it was not possible to keep this latter characteristics constant for all the samples. For instance, the maximum sulfonation rate depends on the grafting density: the most dense brushes (obtained with the shortest chains, $N = 63$) cannot be sulfonated above 45%. Therefore, it was important to determine to which extent this variation could influence the brush structure. However, the sulfonation rate could vary only in a limited range: from 30% to 65%. Indeed, below 30%, the poly(styrenesulfonate sodium salt) is not water-soluble and the (soft) sulfonation method we used does not allow a sulfonation rate higher than 65%.

Figure 8a shows the density profile obtained for different sulfonation rates, with brushes of the same chain length ($N = 310$) and similar grafting density. It appears that the more the brush is charged, the more the chains are extended. This is confirmed by a quantitative analysis (Figure 8b). We observe that the variation of the mean thickness h with the sulfonation rate is compatible with the theoretical prediction $h \approx \alpha^{1/2}$ (cf. eq 1). However, it must be recalled that these data were obtained in a limited range of sulfonation rate (and thickness).

The profile shape can be analyzed in more detail. The differences between the three density profiles in Figure 8a are not very pronounced: they are all rather gently sloped and extend far in the bulk. Nevertheless, it seems that when the sulfonation rate is low, the density profile tends to be structured in two layers: the first is a dense layer near the surface (its thickness and its mean volume fraction $\bar{\phi}$ are, respectively, about 250 Å and 40% for the less sulfonated sample), and the second, far from the surface, is more dilute (thickness ≈ 250 Å and $\bar{\phi} \approx$

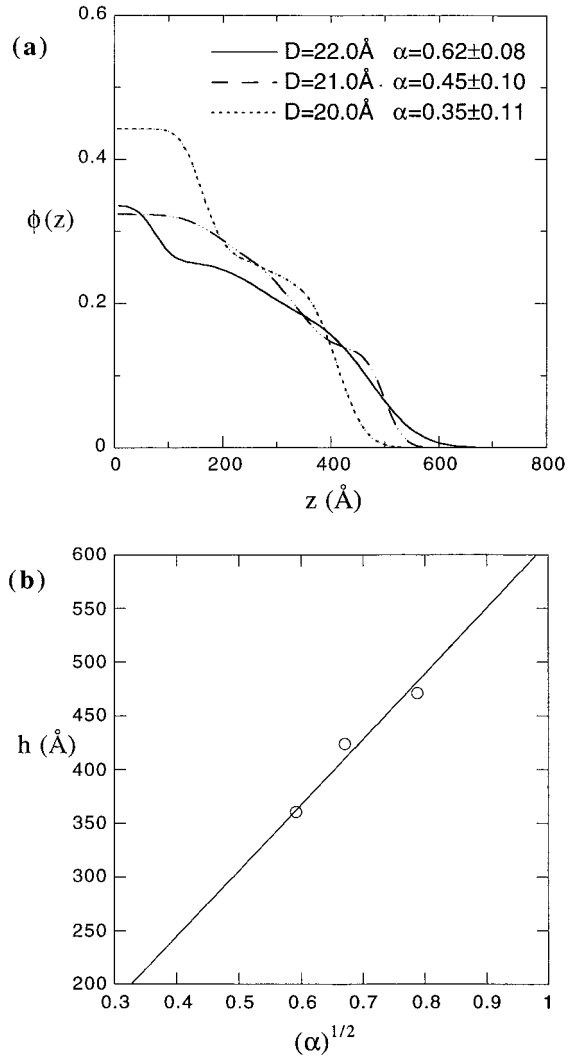

Figure 8. (a) Monomer volume fraction profile for various sulfonation rates α. The PSSNa brushes have the same polymerization index $N = 310$ and similar grafting density. (b) Variation of the mean thickness h (Å) as a function of $\alpha^{1/2}$.

15%). The dense zone might correspond to hydrophobic domains. There are two possible explanations for the existence of such hydrophobic domains: either they are the less sulfonated parts of the chains (randomly distributed along the backbone) or they might be due to globule formation. Globule formation has been proposed by Dobrynin et al.[31] to describe the conformation of "hydrophobic" polyelectrolyte chains: the most favorable conformation of a single chain is to form a string of beads (the "globules"). This would result from a compromise between the elastic free energy, the electrostatic repulsion and the interfacial tension with water. In that sense, this conformation is reminiscent of the Rayleigh instability. The number and the size of the globules depend on the charge rate, the ionic strength, the interfacial tension between water and the hydrophobic monomers, and so on. When decreasing the charge rate, the number of monomers involved in the globules increases. For free chains, the globules are located everywhere along the backbone. This study can be extended to the semidilute case. The model of Dobrynin et al. could also apply to our brushes; however, the globules would form preferentially close to the solid surface because it would allow a gain in interfacial energy. This second explanation accounts qualitatively for our observations and seems to be more reasonable than the first one (less sulfonated domains) because the chains do not need to fold up in order to bring their hydrophobic domains near the solid surface.

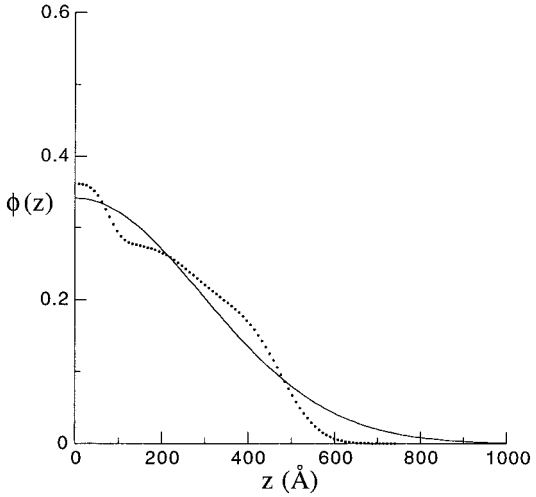

Figure 9. Comparison of the monomer volume fraction profile of a PSSNa brush ($N = 310$, $D = 22.0$ Å, $\alpha = 0.62 \pm 0.08$) in D_2O (dotted line; same data as in Figure 5) with a Gaussian (solid line).

Shape of the Monomer Volume Fraction Profile: Comparison with Theory. In the osmotic regime, theory predicts that the monomer volume fraction profile $\phi(z)$ of a polyelectrolyte brush is Gaussian (for sufficiently large N). However, this result is based on simplified views: for instance, the solid surface is assumed to be perfectly neutral and no hydrophobic interaction is taken into account. It is not clear whether such a description can apply to our samples and to what extent the shape of $\phi(z)$ is modified by these interactions. Nevertheless, a comparison with theory might be relevant in the case of the sample of following characteristics: $N = 310$, $D = 22.0$ Å, and $\alpha = 0.62 \pm 0.08$; because D is small compared to the radius of gyration, it is not altered by a consolidation layer and the degree of sulfonation is high, which should minimize the formation of globules.

No simple analytical forms (Gaussian, step function, or exponential) fit the reflectivity data very well, especially in the "high" k range ($k > 0.015$ Å^{-1}), which is sensitive to the details of the monomer volume fraction profile. This is why we introduced the "layered" model described above, which can account for any regular shape of monomer volume fraction profile, provided the number of layers is sufficiently high. Experimentally, it appears that three layers are enough to describe all our data. Figure 5b gives an idea of the resolution of our reflectivity experiment, translated in terms of $\phi(z)$. At this level, if the best monomer volume fraction profile obtained with the layered model is compared with the theoretical prediction (Gaussian form) (cf. Figure 9), significant deviations are observed, although the agreement is qualitatively good.

Effect of the Consolidation on the Brush Structure. As explained above, it was necessary to consolidate the brushes when their grafting density was relatively low and the molecular weight of the polymer was high (namely, for $N = 1096$). This was achieved by grafting oligomers whose role was to protect the anchoring points of the long (grafted) chains. Although this oligomer carpet is not directly "visible" to neutrons (because it is contrast matched to D_2O), its presence

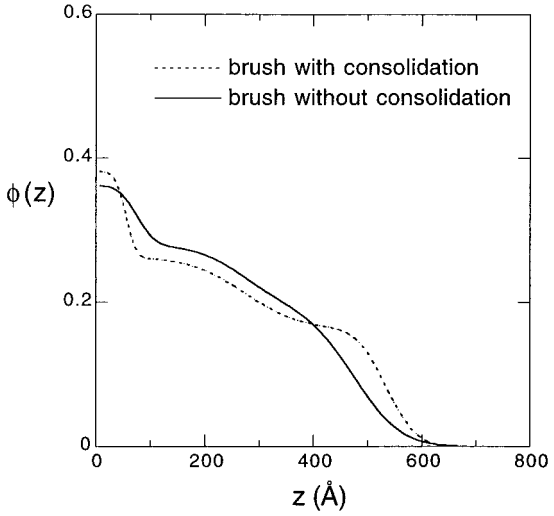

Figure 10. Monomer volume fraction profile of a brush without consolidation (solid line characteristics: $N = 310$, $D = 22.0$ Å, and $\alpha = 0.62 \pm 0.08$ with the same data as in Figure 5) and a brush after consolidation, of similar characteristics (dashed line characteristics: $N = 310$, $D = 21.2$ Å, and $\alpha = 0.60 \pm 0.08$).

might be detected indirectly if it disturbs the brush profile. This effect can be evaluated, to some extent, by comparing two samples of similar characteristics, with only one of the two being consolidated (Figure 10). It has to be noted that this evaluation cannot be done on samples whose grafting density is relatively low, because they are not robust enough to be observed by NR, as mentioned above. In Figure 10, we can notice that the oligomer carpet has an influence only close to the solid surface. In this region, because the monomer volume fraction is increased (due to the "invisible" oligomers), the formation of hydrophobic globules is promoted. Nevertheless, this perturbation is localized within the first 60 Å. We assume that this remains valid for all the consolidated brushes, especially for those at low grafting density.

Effect of the Grafting Density on the Brush Structure. Figure 11a shows the concentration profile of (consolidated) PSSNa brush as a function of the grafting density, with all of the other characteristics being kept constant (chain length $N = 310$, sulfonation rate $\alpha = 0.60 \pm 0.08$). It can be seen that both the maximal extension and the mean thickness are about the same for all of the four samples ($h_{max} \approx 700$ Å and $h \approx 450$ Å). h is more than twice as large as the mean thickness of the corresponding neutral brush in good solvent; the thickness of a PS brush varies from 160 to 230 Å for $D = 21.0$ to 29.0 Å and $N = 310$.[32] We can include the data of Figure 8b and plot $h/\alpha^{1/2}$ as a function of the distance between two anchoring points D as shown in Figure 11b. We observe that the mean thickness $h/\alpha^{1/2}$ does not depend on the grafting density. This result characterizes the osmotic regime that has been predicted for dense and highly charged polyelectrolyte brushes. h does not depend on σ because each chain is stretched by the osmotic pressure due to its own counterions.

The discussion of the density profile shape is again complicated by the presence of a quite dense layer close to the solid surface. This dense proximal layer is mostly due to the oligomer carpet that protects the anchoring points, as seen above. If we examine the rest of the profile, we can observe that the shape of the density

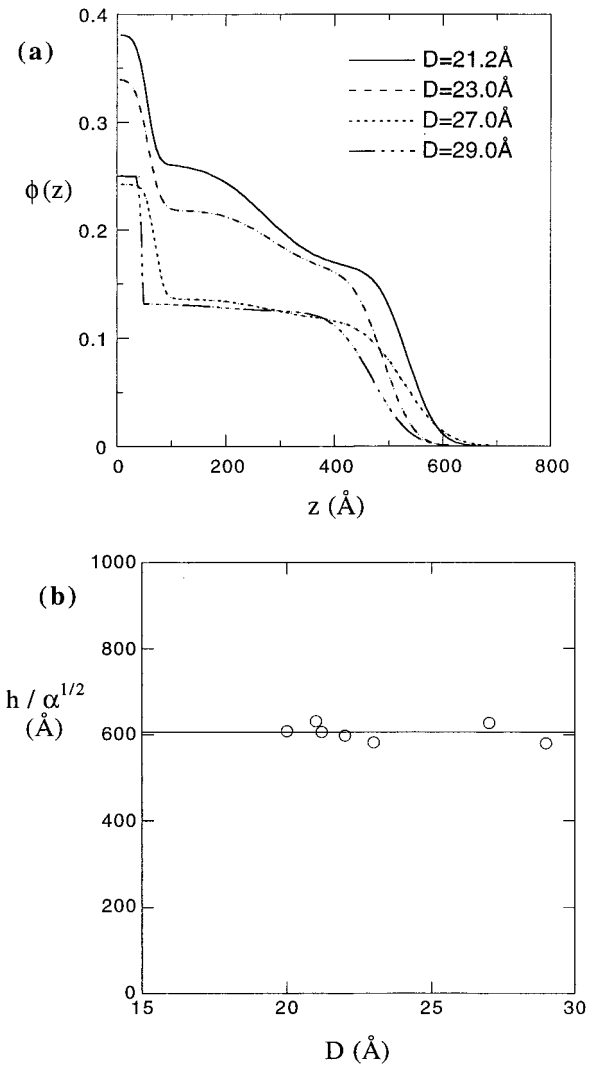

Figure 11. (a) Monomer volume fraction profile for various distances between anchoring points D. The PSSNa brushes have the same polymerization index $N = 310$ and the same sulfonation rate $\alpha = 0.60 \pm 0.08$. (b) Variation of $h/\alpha^{1/2}$ as a function of D.

profile seems to change with the grafting density. As D increases, $\phi(z)$ tends to be a step function. This result is quite surprising, especially because it is exactly the opposite of what is observed for neutral brushes in good solvent. Nevertheless, one can notice that theory predicts such a stepwise density profile for weakly charged brushes.[14−15]

Chain Length Effect. The effect of chain length on the brush structure has also been studied. The reflectivity data corresponding to the samples with $N = 63$ and 1100 are shown in parts a and b, respectively, of Figure 12, and their respective volume fraction profiles are shown in Figure 12c. The two brushes with the longest chains ($N = 310$ and 1100) are consolidated by an oligomer carpet; however, we will consider as we did above that the perturbation induced by this dense protection layer is limited to the first 60 Å, close to the solid surface. For each sample of this part, the grafting density and the sulfonation rate α are as high as possible; this means that the distance between grafting points D and α can differ from one sample to one another. (Experimentally, it is observed that the maximum grafting density decreases with N, whereas the maximum sulfonation rate increases with N). However,

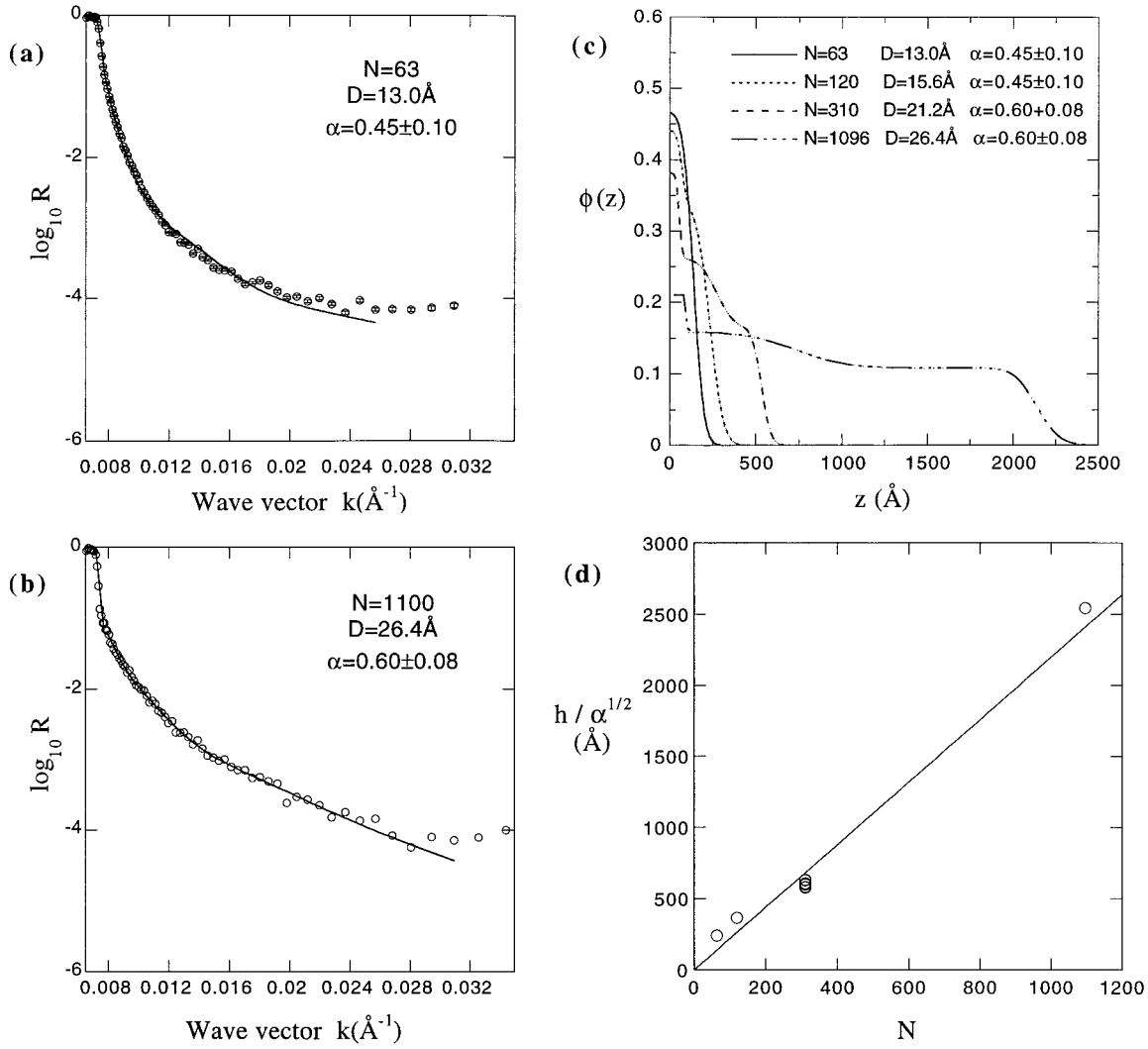

Figure 12. (a) Reflectivity curve of a PSSNa brush in D_2O for $N = 63$. (b) Same curve as in part a but for $N = 1100$. (c) Monomer volume fraction profile of PSSNa brushes of different chain length in D_2O. (d) Variation of $h/\alpha^{1/2}$ as a function of the polymerization index N.

it is still possible to compare these samples because as shown previously, for a given N, the mean thickness h does not depend on D and it is proportional to $\alpha^{1/2}$. Therefore, it is justified to plot $h/\alpha^{1/2}$ versus N. We can observe in Figure 12d that $h/\alpha^{1/2}$ is proportional to N with a factor of proportionality equal to 2.2 Å, comparable to a monomer size. This result is in agreement with the theoretical scaling law $h = Na\alpha^{1/2}$ (eq 1) characteristic of polyelectrolyte brushes in the osmotic regime.

If the brush maximum extension is considered, it can be noticed that for $N = 63$ h_{max} corresponds to the length of a fully stretched chain $L = Na$ (with $a = 5.1$ Å, calculated from the PSSNa density $d = 1.97$ g/cm^3). For larger N, h_{max}/Na decreases while N increases. Therefore, there are two results that appear rather contradictory: h is a linear function of N, but h_{max} does not increase proportionally to N. However, it is possible to reconcile these two observations by considering the shape of the density profile: it is rather close to a step function for brushes made with long chains (of relatively low grafting density), whereas it is much more rounded for short chain brushes (of higher grafting density). To our knowledge, this is not well accounted for by theory.

Counterion Distribution. We have seen that grafted polyelectrolyte chains are strongly stretched in pure water. The interface thickness is proportional to the number of monomers and does not depend on the grafting density: $h \approx Na\alpha^{1/2}$, in agreement with the theoretical prediction in the osmotic regime. This has been interpreted by considering that each chain is stretched by the osmotic pressure of its own counterions. This implies that the counterions are confined inside the brush to ensure a highly local electroneutrality. We have tested this scheme by determining the counterion density profile.[33] As explained above, this experiment was done under contrast match condition using a poly(styrenesulfonate tetramethylammonium) brush. The poly(styrenesulfonate) backbone was 96% deuterated to be "invisible" in D_2O to neutrons; its characteristics ($N = 300$, $D = 21.9$ Å, and $\alpha = 0.40 \pm 0.10$) are comparable to those of a protonated brush already studied; cf. Figure 8a ($N = 310$, $D = 21.0$ Å, and $\alpha = 0.45 \pm 0.10$). The reflectivity curve of the (protonated) tetramethylammonium counterions[34] and the corresponding density profile that best fits the data are reported in Figure 13. This latter has been normalized to take into account the difference in molecular volume between styrenesulfonate and tetramethylammonium. Hence, the density profiles in terms of charge distribution can be directly compared. It turns out that the counterion profile follows quite closely the backbone profile; this means that most of

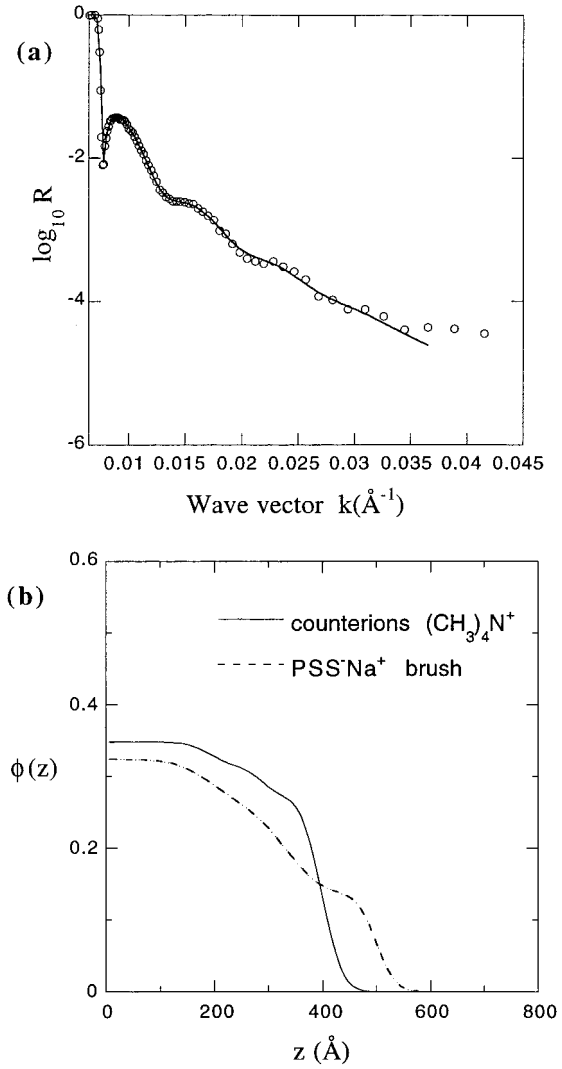

Figure 13. (a) Reflectivity curve of a poly(styrenesulfonate tetramethylammonium salt) brush (characteristics: $N = 300$, $D = 21.9$ Å, and $\alpha = 0.40 \pm 0.10$). (b) Distribution of tetramethylammonium counterions (corresponding to the data shown in part a compared to the monomer volume fraction of a poly(styrenesulfonate sodium salt) brush (characteristics: $N = 310$, $D = 21.0$ Å, and $\alpha = 0.45 \pm 0.10$).

the counterions are confined inside the brush and the local electoneutrality scheme is rather well confirmed.

PSSNa Brushes in Salt Solutions. We have observed that the grafted PSSNa chains are extremely stretched in pure water due to the electrostatic repulsion between charged monomers. What happens to the density profile if we add some salt in the bulk to screen this repulsion?

For low salt concentrations (0.01 and 0.1 mol/L of NaCl), the PSSNa brush has almost the same reflectivity curve as it does in pure water, which means that the profiles are quite similar (Figure 14). (Incidentally, these experiments give another estimate, an upper bound, of the reproducibility of our experiments.) This is not really surprising because the bulk salt concentration remains smaller than the inner concentration of counterions in the brush ($M_{ci} = 1.4$ mol/L for this sample).[35] Under this condition, we are still in the osmotic regime: the added electrolytes are not able to screen the electrostatic repulsion into the brush, and the chains remain strongly stretched.

For higher salt concentrations, the reflectivity curve is modified significantly. In Figure 15a, the data of a

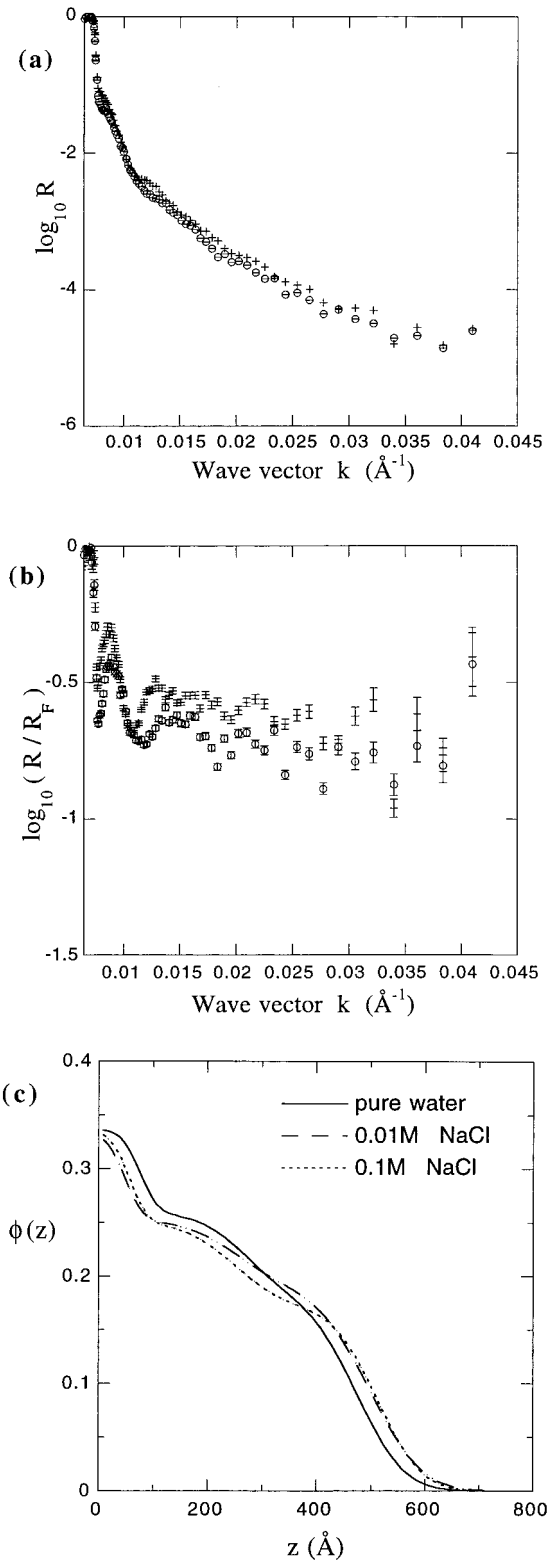

Figure 14. (a) Reflectivity curve of a PSSNa brush in pure D_2O (⊖) and in D_2O at 0.1 M NaCl (+). The brush has the following characteristics: $N = 310$, $D = 22.0$ Å, and $\alpha = 0.62 \pm 0.08$. (b) Same curve as in part a but in the representation $\log_{10} R/R_F$ vs k. (c) Monomer volume fraction profiles that best fit the data shown in parts a and b. The result obtained for 0.01 M NaCl has been added.

PSSNa brush in pure water and in 5 mol/L NaCl solution[36] are compared. The $\log_{10} R/R_F$ versus k representation (Figure 15b) highlights the oscillations of the reflectivity curves that look like interferences between the two edges of the polyelectrolyte brush. The

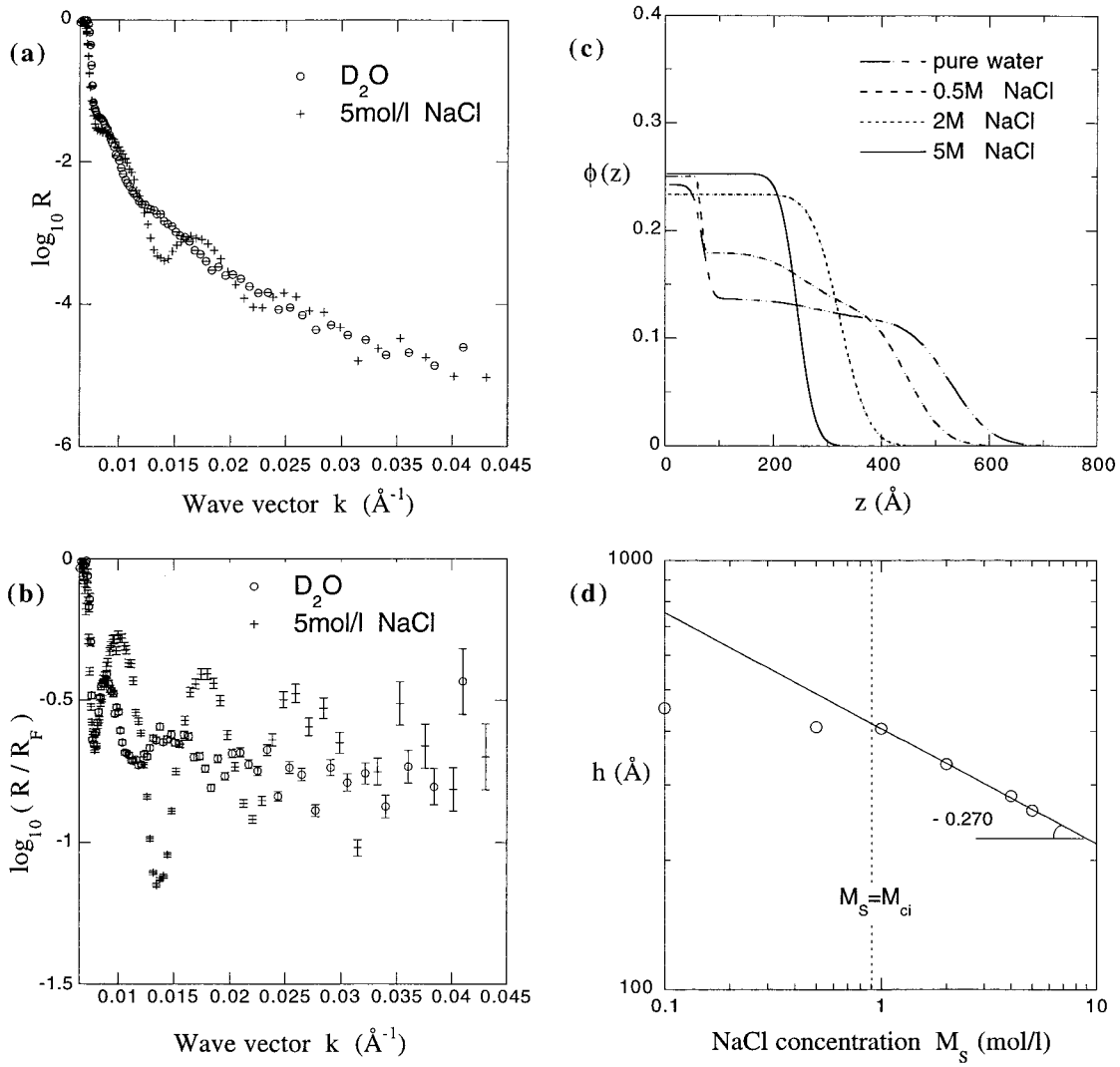

Figure 15. (a) Reflectivity curve of a PSSNa brush in D_2O and in 5 mol/L NaCl solution. The brush characteristics are as follows: $N = 310$, $D = 27.0$ Å, and $\alpha = 0.60 \pm 0.08$. (b) Same curve as in part a but in the representation R/R_F vs k. (c) Monomer volume fraction profile of the same brush as in part a for various NaCl concentrations in the strong screening regime. (d) Variation of the mean thickness h as a function of the added salt concentration M_S.

period and the amplitude of the oscillations are larger in 5 mol/L NaCl than those in pure water. It means that at high salt concentrations the brush thickness is smaller and the profile is closer to a step function. This can be clearly seen with the result of the fit to the reflectivity data shown in Figure 15c: the polyelectrolyte layer shrinks more and more as the ionic strength is increased. In Figure 15d, the layer thickness h is plotted as a function of the salt concentration M_S. This plot shows clearly two regimes: a first regime at low NaCl concentration where h is rather constant and a second regime where h decreases with M_S for $M_S \geq 1$ mol/L. In the regime where h is constant, the NaCl concentration is smaller than the inner concentration of counterions ($M_{ci} = 0.9$mol/L for this sample): this corresponds to the osmotic regime described before. For $M_S > M_{ci}$, h decreases with M_S as $h = 407.2M_S^{-0.27\pm0.01}$ or $h = 148.1\varphi_S^{-0.27\pm0.01}$ (φ_S is the added salt volume fraction). This result compares quite favorably with the theory (see eq 3): the experimental exponent is quite close to that predicted, $-1/3$, and from the numerical prefactor, we can deduce a typical size $a = 2.9$ Å, which is again a reasonable value for a monomer size. Concerning the profile shape, we can observe that the dense proximal layer induced by the presence of the protective oligomer carpet seems to disappear as the ionic strength increases. This results probably from the shrinking of the layer: it becomes progressively more homogeneous.

Table 3. Brush Thickness at High Salt Concentration (5 M NaCl)

polym. index, N	D (Å)	α	h (Å)
63	13.0	0.45	115
310	22.0	0.62	306
310	27.0	0.60	261
1096	26.4	0.60	1002

The effects of chain length and grafting density have been investigated in more detail at a fixed salt concentration, − 5 mol/L in NaCl,[36] although this study is far from being exhaustive. From the few samples we examined, we can say that the brush thickness h seems to vary with the chain length and the distance between grafting points in a manner similar to that predicted by eq 3, namely, h (Å) $\propto ND^{-0.67}$ (cf. Table 3 and Figure 16). However, a definite conclusion cannot be drawn because of insufficient data. Nevertheless, the comparison of the salt effect on a polyelectrolyte brush and the solvent quality effect on a neutral polymer brush may be interesting. The thickness of the PSSNa brush ($N = 310$, $D = 22.0$ Å) is 490 Å (respectively, 260 Å) in pure

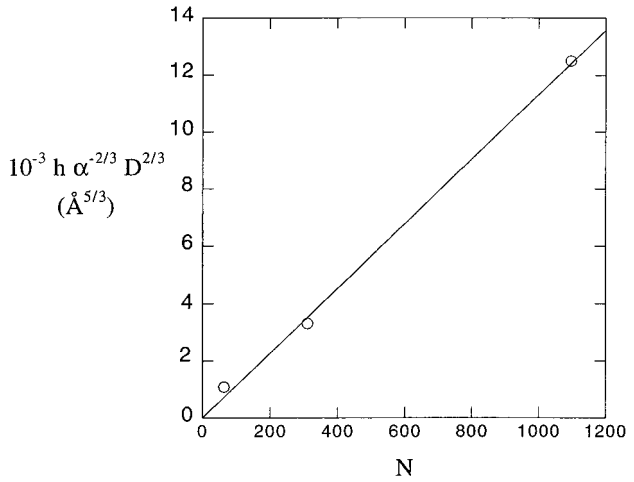

Figure 16. Variation of the mean thickness (normalized by $\alpha^{-2/3}D^{2/3}$) as a function of N, for PSSNa brushes in 5 mol/L NaCl solution. The corresponding data and the other characteristics are given in Table 3.

water (respectively, in 5 mol/L NaCl), whereas the thickness of the equivalent PS brush should be 260 Å (respectively, 120 Å) in good solvent (respectively, in poor solvent).[32] Thus, it appears that the addition of salt has an effect similar to that of a change in solvent quality: the brush shrinks by a factor of 2. However, the polyelectrolyte chains do not collapse even in 5 mol/L NaCl; they are as stretched as neutral chains in good solvent (the thickness is comparable). Although the PSSNa chains have some hydrophobic character, there is still a repulsive excluded volume interaction between the counterions that remains even if the long-range electrostatic repulsion is completely screened. This explains why the chains are stretched and why polyelectrolyte brushes follow the same scaling law in the strong screening regime as do polymer brushes in good solvent (the excluded volume parameter being proportional to φ_S^{-1}).

Finally, a few experiments have been done with a divalent salt. Figure 17a shows the profile of a poly(styrenesulfonate calcium salt) brush in $CaCl_2$ solutions of different concentration (all samples were consolidated with deuterated oligomers). As has been observed for the monovalent salt NaCl, the poly(styrenesulfonate calcium salt) layer shrinks progressively as the $CaCl_2$ concentration increases. Quantitatively, $h \approx M_S^{-0.28}$ This law is similar to the result obtained for NaCl. The valence difference must be taken into account to compare the effect of NaCl and $CaCl_2$. For the two profiles obtained with the same brush in 2 mol/L NaCl and 1 mol/L $CaCl_2$ shown in Figure 17b, there are approximately the same number of charges per unit volume. The screening of the electrostatic interaction looks nearly as efficient for 1 mol/L $CaCl_2$ as for 2 mol/L NaCl: the brush thickness is comparable (335 Å in 2 mol/L NaCl and 303 Å in 1 mol/L $CaCl_2$). However, in $CaCl_2$, the brush is a bit denser and a depletion layer appears near the surface; this can also be observed in Figure 17a. This slight difference might be due to chain cross-links induced by the divalent ions. The cross-links would be responsible for the further shrinkage. However, the chains cannot come close to the surface because of the steric exclusion due to the deuterated oligomers, which likely form a cross-linked network themselves. (By comparison with the data obtained with the shortest protonated polymer, $N = 63$, cf. Figure 12b, the volume

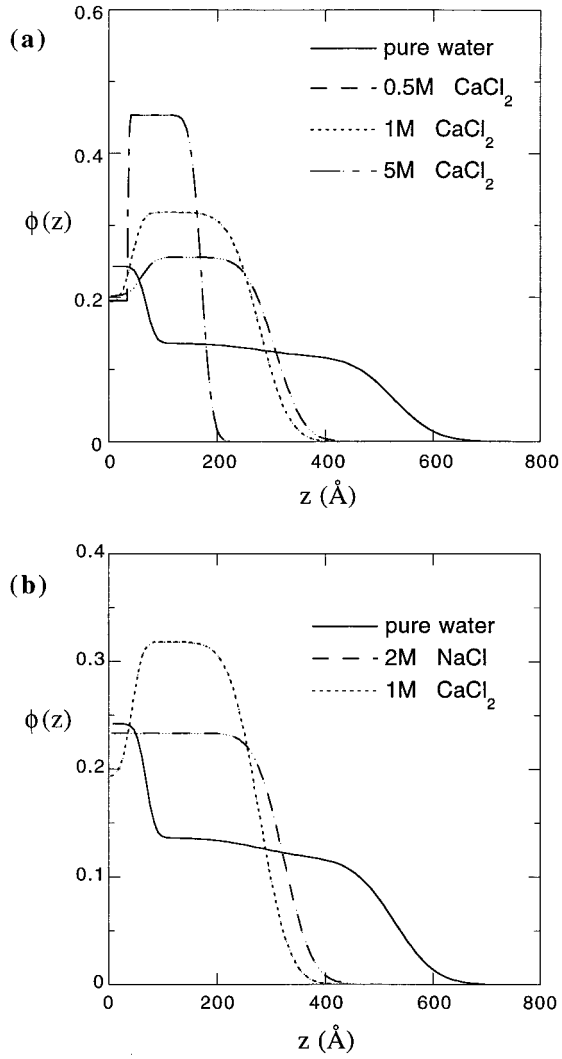

Figure 17. (a) Monomer volume fraction profile of a poly(styrenesulfonate calcium salt) brush for various $CaCl_2$ concentrations (in the strong screening regime). The brush has the following characteristics: $N = 310$, $D = 27.0$ Å, and $\alpha = 0.60 \pm 0.08$. (b) Comparison between the effect of adding NaCl or $CaCl_2$ on the brush monomer volume fraction profile.

fraction of the deuterated oligomer layer can be estimated to be 50%.) Nevertheless, the cross-link effect is probably weak compared to the charge-screening effect.

Conclusion

In this paper, we have studied the interfacial structure of polyelectrolyte brushes in aqueous solutions. We have observed that the chains are strongly stretched due to the electrostatic repulsion between charged monomers; in some cases, they are fully extended. The characteristic thickness of the brush is proportional to the chain length but does not depend on the grafting density. These results are in agreement with the theoretical predictions for polyelectrolyte brushes at high charge and high grafting density in the osmotic regime where the chains can be viewed as if each of them were stretched by the osmotic pressure due to their own counterions. These counterions are found experimentally to be confined inside the polyelectrolyte layer to ensure a highly local electroneutrality. The effect of adding salt in solution has also been investigated. We have shown that the added electrolytes have no influence on the brush profile as long as their

concentration is less than the inner counterion concentration. On the other hand, for higher salt concentration, the polyelectrolyte layer shrinks but never collapses. If a divalent salt is used, there might be some cross-link effects but they are weaker than the charge-screening effect.

Among the extensions that we can suggest from this study, it would be interesting to investigate the wetting properties of such polyeletrolyte brushes. There might be a wetting transition induced by the salt concentration. To our knowledge, nothing has yet been done in this area. It would also be interesting to take advantage of the methods we have used in this study to address other questions: for instance, it might be possible to observe directly by neutron reflectivity the action of a restriction enzyme onto an adsorbed protein.

References and Notes

(1) Pincus, P. *Macromolecules* **1991**, *24*, 2912.
(2) Wittmer, J.; Joanny, J. F. *Macromolecules* **1993**, *26*, 2691.
(3) Zhulina, E. B.; Borisov, O. V.; Priatmitsyn, V. A. *J. Colloid Interface Sci.* **1990**, *137*, 495.
(4) Borisov, O. V.; Zhulina, E. B.; Birshtein, T. M. *Macromolecules* **1994**, *27*, 4795.
(5) Zhulina, E. B.; Borisov, O. V.; Birshtein, T. M. *J. Phys. II* **1991**, *1*, 521.
(6) Ross, R. S.; Pincus, P. *Macromolecules* **1992**, *25*, 2177.
(7) Zhulina, E. B.; Birshtein, T. M.; Borisov, O. V. *Macromolecules* **1995**, *28*, 1491.
(8) Misra, S.; Mattice, W.; Napper, D. *Macromolecules* **1994**, *27*, 7090.
(9) Zhulina, E. B.; Borisov, O. V. *Macromolecules* **1996**, *29*, 2618.
(10) Misra, S.; Varanasi, S.; Varanasi, P. P. *Macromolecules* **1989**, *22*, 4173.
(11) Zhulina, E. B.; Borisov, O. V.; Birshtein, T. M. *J. Phys. II* **1992**, *2*, 63.
(12) Israëls, R.; Leermakers, F. A. M.; Fleer, G. J.; Zhulina, E. B. *Macromolecules* **1994**, *27*, 3249.
(13) Pryamitsyn, V. A.; Leermakers, F. A. M.; Fleer, G. J.; Zhulina, E. B. *Macromolecules* **1996**, *29*, 8260.
(14) Zhulina, E. B.; Borisov, O. V. *J. Chem. Phys.***1997**, *107*, 5952.
(15) Borisov, O. V.; Zhulina, E. B. *J. Phys. II* **1997**, *7*, 449.
(16) Harden, J. L. *Macromolecules* **1997**, *30*, 1179.
(17) Harden, J. L. *Macromolecules* **1997**, *30*, 5930.
(18) Amiel, C.; Sikka, M.; Schneider, J. W.; Tsao, J. H.; Tirrell, M.; Mays, J. W. *Macromolecules* **1995**, *28*, 3125. See also: Kelley, T. W.; Schorr, P. A.; Johnson, K. D.; Tirrell, M.; Frisbie, C. D. *Macromolecules* **1998**, *31*, 4297.
(19) Walter, H.; Harrats, C.; Müller-Buschbaum, P.; Jérôme, R.; Stamm, M. *Langmuir* **1999**, *15*, 1260.
(20) Guenoun, P.; Schalchli, A.; Sentenac, D.; Mays, J. W.; Benattar, J. J. *Phys. Rev. Lett.* **1995**, *74*, 3628. See also: Guenoun, P. et al. *Phys. Rev. Lett.* **1998**, *81*, 3872.
(21) Mir, Y.; Auroy, P.; Auvray, L. *Phys. Rev. Lett.* **1995**, *75*, 1863.
(22) (a) Meier, L. P.; Shelden, R. A.; Caseri, W. R.; Suter, U. W. *Macromolecules* **1994**, *27*, 1637. (b) Jordan, R.; Ulman, A. *J. Am. Chem. Soc.* **1998**, *120*, 243. (c) Prucker, O.; Rühe, J. *Macromolecules* **1998**, *31*, 592. (d) Husseman M. et al. *Macromolecules* **1999**, *32*, 1424. (e) Jordan, R.; Ulman, A.; Kang, J. F.; Rafailovich, M. H.; Sokolov, J. *J. Am. Chem. Soc.* **1999**, *121*, 1016.
(23) Biesalski, M.; Rühe, J. *Macromolecules* **1999**, *32*, 2309.
(24) (a) Alexander, S. *J. Phys.* **1977**, *38*, 977. (b) de Gennes, P.-G. *Macromolecules* **1980**, *13*, 1069.
(25) Milner, S. T.; Witten, T. A.; Cates, M. E. *Macromolecules* **1988**, *21*, 2610.
(26) Ou Ramdane, O.; Auroy, P.; Silberzan, P. *Phys. Rev. Lett.* **1998**, *80*, 5141.
(27) Tillman, N.; Ulman, A.; Schildkraut, J. S.; Penner, T. L. *J. Am. Chem. Soc.* **1988**, *110*, 6136.
(28) Makowski, H. S.; Lundberg, R. D.; Singhal, G. S. U.S. Patent 3870841, 1975.
(29) Russell, T. P. *Mater. Sci. Rep.* **1990**, *5*, 171.
(30) Kent, M. S.; Lee, L. T.; Factor, B. J.; Rondelez, F.; Smith, G. S. *J. Chem. Phys.* **1995**, *103*, 2320.
(31) Dobrynin, A. D.; Rubinstein, M.; Obukhov, S. P. *Macromolecules* **1996**, *29*, 2974.
(32) These values are calculated from the experimental results reported in: Auroy, P.; Mir, Y.; Auvray, L. *Phys. Rev. Lett.* **1992**, *69*, 93.
(33) Tran, Y.; Auroy, P.; Lee, L. T.; Stamm, M. *Phys. Rev. E.*, submitted for publication.
(34) It should be mentioned that the counterion distribution has been determined in the presence of 0.1 M tetramethylammonium chloride in solution. This bulk concentration is much less than the inner counterion concentration (on the order of 1 M). It does not change the brush profile, as shown in the next paragraph. In the absence of tetramethylammonium chloride in solution, we observe a slow disappearance of the counterions. This is attributed to exchanges with other ions (most likely sodium) that are present in the bulk at a trace level. More detail will be given in a forthcoming publication.
(35) The inner concentration of counterions is calculated by considering that all the counterions are trapped in the brush. It corresponds to the concentration of charged monomers. $\phi_{ci} = N\alpha a^3/hD^2$ and M_{ci} (mol/L) $= N\alpha/hD^2N_A$, where N_A is Avogadro's number and a (monomer size) is supposed to be the same for the counterion.
(36) The 5 mol/L NaCl concentration is close to the solubility limit of NaCl in water.

MA990443R